THE JOURNAL OF COMPARATIVE NEUROLOGY 438:50–65 (2001)

Distribution of Substance P and Neurokinin-1 Receptor Immunoreactivity in the Suprachiasmatic Nuclei and Intergeniculate Leaflet of Hamster, Mouse, and Rat

HUGH D. PIGGINS,* RAYNA E. SAMUELS, ANDREW N. COOGAN, AND DAVID J. CUTLER
School of Biological Sciences, University of Manchester, Manchester M13 9PT, United Kingdom

ABSTRACT

The circadian pacemaker in the hypothalamic suprachiasmatic nuclei (SCN) receives photic information directly via the retinohypothalamic tract (RHT) and indirectly from retinally innervated cells in the thalamic intergeniculate leaflet (IGL) that project to the SCN. Using standard immunohistochemical methods, we examined the presence and distribution of substance P (SP) and the neurokinin-1 receptor (NK-1) in the SCN and IGL of rat and determined whether the patterns of immunostaining generalized to the SCN and IGL of Syrian hamster, Siberian hamster, and mouse. Terminals immunoreactive for SP were sparse within the SCN of Siberian and Syrian hamsters and mouse but were intense in the ventral, retinally innervated portion of the rat SCN. Immunostaining for the NK-1 receptor was mainly absent from the SCN of hamster and mouse. In contrast, a plexus of NK-1-ir cells and processes that was in close proximity to SP-ir terminals was found in the ventral SCN of the rat. Substance P-ir terminals were observed in the IGL of all four species, as were NK-1-ir cells and fibres. Double-labelled IGL sections of hamster or rat revealed SP-ir terminals in close apposition to NK-1-immunostained cells and/or fibres. These data indicate that SP could be a neurotransmitter of the RHT in rat, but not in hamster or in mouse, and they highlight potential species differences in the role of SP within the SCN circadian pacemaker. Such species differences do not appear to exist at the level of the IGL, where SP-ir and NK-1-ir were similar in all species studied. J. Comp. Neurol. 438:50–65, 2001.

Indexing terms: circadian rhythm; immunohistochemistry; rodent; hypothalamus; lateral geniculate nucleus; retinohypothalamic tract

Circadian rhythms in physiological and behavioural processes are a product of the activity of an internal circadian pacemaker (or clock) and the synchronization of this clock's activity with recurring environmental time cues called Zeitgebers. The dominant mammalian circadian clock is located in the suprachiasmatic nuclei (SCN) of the hypothalamus (Ralph et al., 1990; Silver et al., 1996; van Esseveldt et al., 2000; Hastings and Maywood, 2000). The SCN clock is entrained to environmental photic information conveyed from the retina to the SCN directly via the monosynaptic retinohypothalamic tract (RHT) and indirectly through the geniculohypothalamic tract (GHT), which arises from cells of the intergeniculate leaflet (IGL) of the visual thalamus (Morin, 1994; Reuss, 1996; Piggins and Rusak, 1999). A critical problem in circadian neurobiology is the identification of neurochemicals contained in the GHT and RHT and determination of the mechanisms by which they alter the activity of cells in the SCN and hence timekeeping processes.

Grant sponsor: MRC; Grant number: G962293N; Grant sponsor: BBSRC; Grant number: 34/S12011.

*Correspondence to: Hugh Piggins, 3.614 Stopford Building, School of Biological Sciences, University of Manchester, Oxford Road, Manchester M13 9PT, UK. E-mail: hugh.piggins@man.ac.uk

Received 31 January 2001; Revised 25 May 2001; Accepted 8 June 2001

Considerable evidence indicates that glutamate is the principal neurotransmitter of the rodent RHT. Electron microscopy studies have shown that glutamate is found in RHT terminals forming synaptic contacts with SCN cells in mouse and rat (Castel et al., 1993; de Vries et al., 1993). In situ hybridization and immunohistochemical experiments have indicated the presence of mRNA and receptor proteins of the N-methyl-D-aspartate (NMDA) and non-NMDA classes of ionotropic glutamate receptors in the rodent SCN (Ebling, 1996; Stamp et al., 1997). Electrophysiological investigations have shown that both NMDA and non-NMDA glutamate receptor antagonists block the excitatory effect of optic nerve stimulation on SCN cells in vitro (Kim and Dudek, 1991), whereas microinjection of these antagonists into the SCN region blocks the phase-resetting effects of light on behavioural rhythms (Rea et al., 1993) as well as photic induction of immediate early genes in the SCN (Abe and Rusak, 1994).

In addition to glutamate, another neurochemical thought to be contained in the RHT is the peptide substance P (SP). Neuroanatomical investigations have revealed SP-immunoreactivity (-ir) in fibres and terminals of the rat SCN (Cuello and Kanazawa, 1978; Ljungdahl et al., 1978). A study that combined neural tract-tracing with immunohistochemistry has demonstrated in the rat that a population of SP-ir retinal ganglion cells projects directly to the SCN (Takatsuji et al., 1991). Subsequent electrophysiological studies have shown that SP activates rat SCN cells in vitro (Shibata et al., 1992; Shirakawa and Moore, 1994) and phase-shifts the electrical activity of rat SCN neurones in a manner resembling the effects of light pulses on rodent behavioural rhythms (Shibata et al., 1992). Although SP activates Syrian hamster SCN cells in vitro (Piggins et al., 1995), microinjection of SP into the SCN region in vivo fails to evoke significant phase shifts in hamster circadian activity rhythms (Piggins and Rusak, 1997). Concordant with this in vivo finding, immunohistochemical studies have shown a paucity of SP-ir terminals in the ventral, retinally innervated portion of the SCN in Syrian hamster as well as in mouse (Morin et al., 1992; Hartwich et al., 1994; Silver et al., 1999). Taken in sum, these findings suggest that the role of SP in the rodent circadian pacemaker may vary from species to species.

To determine whether neuroanatomical differences underlie the apparent discrepancies in the role SP may play in circadian processes across species, we examined the distribution of SP-ir and neurokinin-1 receptor immunoreactivity (NK-1-ir)—the receptor thought to mediate the actions of SP on neurones—in the SCN and IGL brain regions of mouse, rat, Syrian hamster, and Siberian hamster.

Abbreviations

3V	third ventricle
AHA	anterior hypothalamic area
DAB	3,3′-diaminobenzidene tetrachloride
dLGN	dorsal lateral geniculate nuclei
GHT	geniculohypothalamic tract
IGL	intergeniculate leaflet
NK-1	neurokinin-1 receptor
OT	optic tract
OX	optic chiasm
RHT	retinohypothalamic tract
SCN	suprachiasmatic nuclei
SP	substance P
vLGN	ventral lateral geniculate nuclei
ZI	zona incerta

MATERIALS AND METHODS

Animals

Four species of adult male rodents were used in this study: Wistar rats (n = 6; Charles River, Margate, Kent, UK), Siberian hamsters (*Phodopus sungorus*; n = 6; Biological Sciences Unit, Manchester, UK), Syrian hamsters (*Mesocricetus auratus* LVG:lak; n = 7; Charles River), and C57BL/6xSV129 mice (n = 6, Biological Sciences Unit). All procedures were carried out in accordance with the UK Animals (Scientific Procedures) Act 1986.

Rats and mice were maintained in a 24-hour light-dark cycle (12 hours light, lights on 07:00), and Syrian and Siberian hamsters were kept in a 24-hour light-dark cycle with 16 hours of light (lights on 07:00). All animals had ad libitum access to food and water. Animals were killed by an overdose of sodium pentobarbital (Pentoject, Animal Care, York, UK: 200 mg/ml; 0.7 ml/animal) during the subjective day and perfused intracardially with 0.9% saline followed by cold (4°C) Zamboni's fixative (4% paraformaldehyde and 15% picric acid in 0.1 M phosphate-buffered saline [PBS], pH 7.4). The brains were removed, postfixed in Zamboni's fixative for 24–48 hours at 4°C, and cryoprotected in a 30% sucrose/PBS (pH 7.4) solution (24–48 hours, 4°C).

Antisera

Substance P-ir was detected using a monoclonal anti-SP antibody raised in rats at a dilution of 1:100 (Harlan-Sera Labs, Loughborough, UK) or a polyclonal anti-SP antiserum raised in rabbits at a dilution of 1:2000 (Affiniti Labs, Exeter, UK). Neurokinin-1 receptor immunoreactivity was investigated using a polyclonal antiserum against the NK-1 receptor, raised in rabbits at 1:5000 dilution (Chemicon, Harrow, UK). Biotinylated goat anti-rat (1:200; Vector Labs, Peterborough, UK) was used as a secondary antibody for the SP monoclonal antibody, and biotinylated goat anti-rabbit (1:400; Vector Labs) was used as a secondary antibody for the SP and NK-1 receptor polyclonal antisera.

Control experiments were performed by omission of the primary or secondary antisera. Specificity of the SP primaries was confirmed in preliminary studies in which the SP monoclonal antibody or SP polyclonal antiserum were preadsorbed with SP (10^{-6} M, 2-hour incubation at room temperature). The control for the NK-1 antisera was preadsorption with a synthetic peptide (10^{-7} M, 2-hour incubation at room temperature) corresponding to the sequence 393–407 (KTMTESSSFYSNMLA) of the C-terminus of the NK-1 receptor (Severn Biotech, Kidderminster, UK).

Sectioning and immunohistochemistry

In the protocol to follow, all rinses and treatments were performed at room temperature, unless otherwise stated. The rinses consisted of three to four changes of PBS and one change of PBS with 0.03% Triton X-100 (PBSx; pH 7.4; 10 minutes each). Primary antisera were diluted in a solution of 2% bovine serum albumin (Sigma, Poole, UK) and 1% normal goat serum (Sigma) in PBSx, and secondary antisera were diluted in PBSx only, unless otherwise

stated. Triton X-100 was excluded from all steps of the protocol when anti-NK-1 primary antiserum was used.

Cryoprotected tissue was rapidly frozen using crushed dry ice on a sledge microtome equipped with a cryostage (Series 8000, Brights Instruments, Huntingdon, UK), cut into 30-μm-thick coronal sections, and collected into PBS. Sets of three sections were taken from the diagonal band of Broca to the retrochiasmatic area (collectively referred to as SCN sections), and another three sets were taken from the arcuate nucleus to the superior colliculus (collectively referred to as IGL sections).

The floating sections were rinsed and incubated in a solution of 0.3% hydrogen peroxide, 20% methanol, and PBSx (20 minutes) to abolish endogenous peroxidase activity. Sections were rinsed, incubated in a blocking solution containing 2% bovine serum albumin and 1% normal goat serum in PBSx (60 minutes), and then incubated with the anti-SP or anti-NK-1 receptor antiserum for 48–72 hours at 4°C with agitation on an orbital shaker.

Sections were rinsed and incubated with the appropriate biotinylated secondary antiserum (90 minutes). The sections were rinsed, incubated in an avidin-biotin immunoperoxidase complex (Vectastain ABC kit, Vector Labs), diluted in PBSx (90 minutes), and rinsed twice in PBS and once in 0.1 M sodium acetate buffer (pH 6.0). The location of antigens was visualized using a 3,3′-diaminobenzidene tetrachloride (DAB) complex (Vectastain peroxidases kit, Vector Labs) either with nickel chromagen that produced a purple/black stain, or without nickel, where a brown stain was observed. Placing the sections back into the acetate buffer stopped the reaction. For dual immunolabelling for SP and the NK-1 receptor, tissue previously immunostained for the NK-1 receptor (with nickel-DAB) was washed, placed into the blocking solution for 30 minutes, and then incubated in rat monoclonal SP antiserum (1:100 dilution) for 48 hours at 4°C. As described above, sections were washed, incubated in the appropriate secondary antiserum, washed, incubated in avidin-biotin immunoperoxidase complex, and visualized using DAB complex (which gave an orange-brown colour).

The sections were rinsed in PBS, mounted onto chrome alum gelatin slides, dried, dehydrated through a series of alcohol concentrations, cleared in Histoclear (National Diagnostics, Hull, UK), and coverslipped with Entellan (Merck, Darmstadt, Germany). Sections were examined under an Olympus BX50 microscope and brain structures described with reference to Paxinos and Watson (1998). Photomicrographs were taken using either an Olympus digital camera (CZ2020) mounted on an Olympus BX50 microscope or an analogue camera mounted on a Leitz Diaplan microscope. Plates were created using Adobe Photoshop 5.0 and Corel Draw 7.0 running on an IBM Pentium PC. Line drawings based on cresyl violet-stained sections through the SCN and IGL were created using Canvas 7.0 SE.

RESULTS

Immunostaining for SP and NK-1 was present in the SCN and IGL regions of all species examined. In general, the pattern of immunostaining for SP was similar with the monoclonal SP antibody and the SP polyclonal antiserum, although the quality of the staining varied. Staining with the polyclonal SP antiserum tended to be darker but less sharp in the SCN region of all four species, whereas at the level of the IGL, the monoclonal antibody gave sharper, more intense staining.

Suprachiasmatic nuclei

Rat. Substance P-ir terminals were observed throughout the rostrocaudal extent of the SCN. The abundance of SP-ir terminals varied from very sparse in the rostral SCN region, to moderately dense in the ventromedial portion of the intermediate region of the SCN (Fig. 1A), to sparse in the caudal SCN (Fig. 3A,E,I). Numerous ovoid SP-ir cell bodies were seen in the ventral aspects of the intermediate regions of the SCN (Fig. 2A), but the quantity of these cells declined throughout the more caudal SCN sections. Moderate to intense SP-ir terminals and fibres were seen throughout the rostrocaudal extent of the hypothalamic region adjacent to the SCN (the anterior hypothalamic area or AHA), but no SP-immunopositive cells were observed at any level of the AHA.

Fibres and neurones expressing NK-1-ir were observed in the AHA surrounding the SCN. The fibres were studded with varicosities, which may be indicative of synaptic interactions. Occasionally these NK-1-ir fibres extended into the outer shell of the dorsolateral SCN (Fig. 1B), where there was also evidence of a small number of NK-1-immunolabelled cell bodies. The numbers of cells and fibres expressing NK-1-ir in the AHA increased rostrocaudally, with the highest density found around the intermediate level of the SCN (Fig. 3A,E,I). A discrete cluster of neurones that exhibited dark NK-1-ir staining was also observed in the ventral area of the SCN. In sections double-labelled for SP and NK-1, SP-ir terminals could be seen in the immediate vicinity of NK-1-ir cell bodies and dendrites within the ventral SCN (Fig. 4A,B).

Syrian hamster. A high density of darkly stained SP-ir terminals was observed surrounding the outer shell of the SCN at all rostrocaudal levels. The AHA contained moderate to intense levels of SP-ir fibre and terminal staining. With the exception of a discrete population of oval-shaped SP-ir neurones in the central region of the intermediate SCN (Fig. 2B), SP-ir was limited to sparse, lightly labelled terminals (Figs. 1C, 3B,F,J).

A large accumulation of NK-1-ir fibres and cell bodies was found surrounding the SCN at all rostrocaudal levels. Numerous fibres from the more densely populated fibrous AHA appeared to project into the periphery of the SCN (Fig. 1D). Aggregations of cell bodies were observed in the dorsolateral region surrounding the SCN, with a smaller number surrounding the ventrolateral regions at intermediate to caudal levels (Fig. 3B,F,J). The density of immunolabelled fibres and cells was moderate to high along the dorsal and lateral extents of the SCN throughout its rostrocaudal aspect. Fibres and terminals immunoreactive for NK-1 were also found adjacent to the third ventricle in the periventricular area. These immunoreactive fibres had an irregular appearance, presumably indicative of synaptic contacts at the swellings. In sections double-labelled for SP and NK-1, SP-ir terminals were observed in close proximity to NK-1-ir perikarya along the dorsolateral border of the SCN as well as to NK-1-ir processes in the central region of the SCN (Fig. 4C,D).

Siberian hamster. A moderate density of SP-ir terminals was observed surrounding the SCN at all rostrocaudal levels. At the intermediate levels of the SCN, a few darkly stained fibres were found in the AHA, dorsal to the SCN. The periventricular region bordering the third ven-

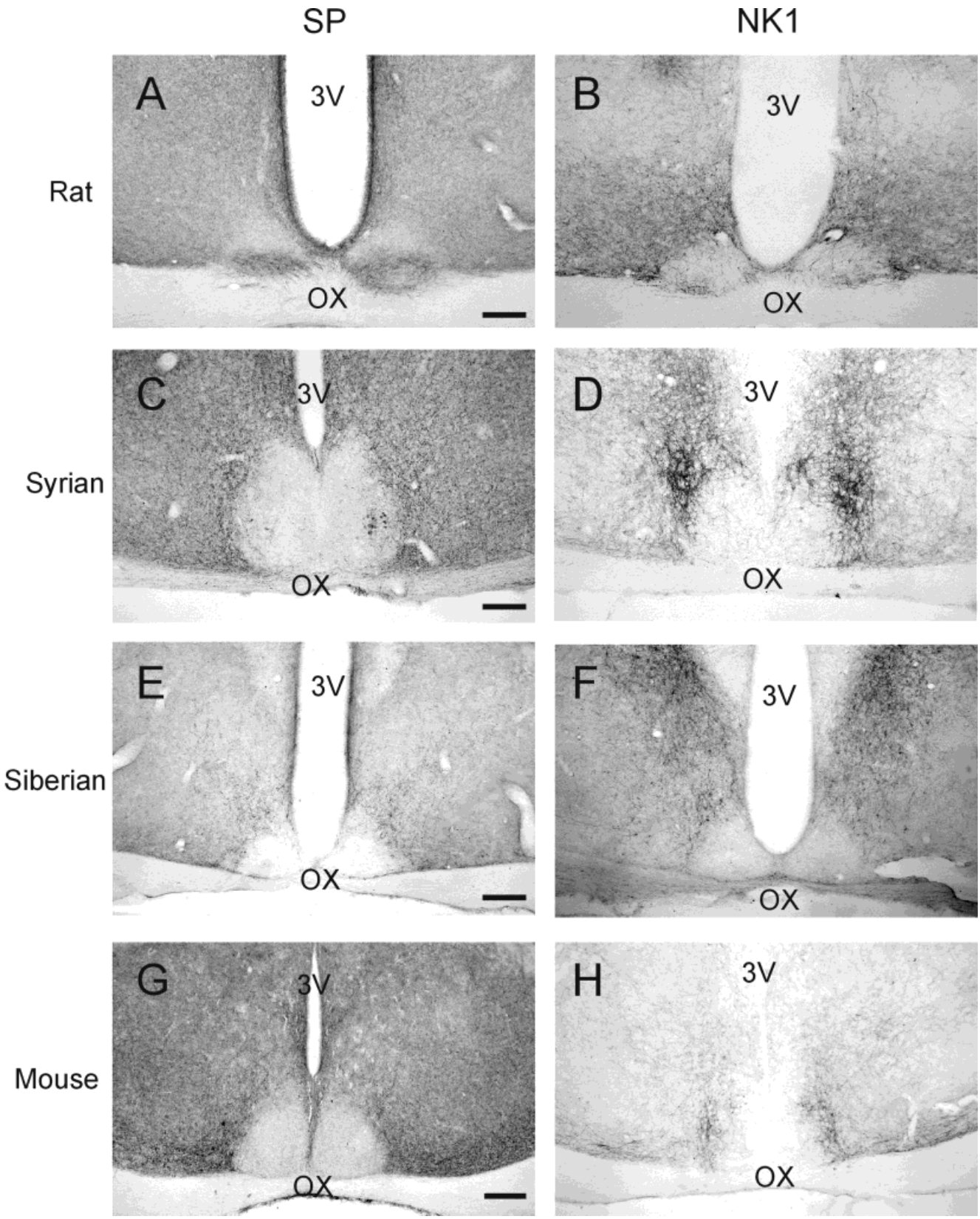

Fig. 1. Low-power photomicrographs showing the pattern of substance P (SP) (**A**,**C**,**E**,**G**) and neurokinin-1 receptor (NK-1) (**B**,**D**,**F**,**H**) immunostaining in the intermediate level of the suprachiasmatic nuclei (SCN) in rat (A,B), Syrian hamster (C,D), Siberian hamster (E,F), and mouse (G,H). Scale bars = 100 μm.

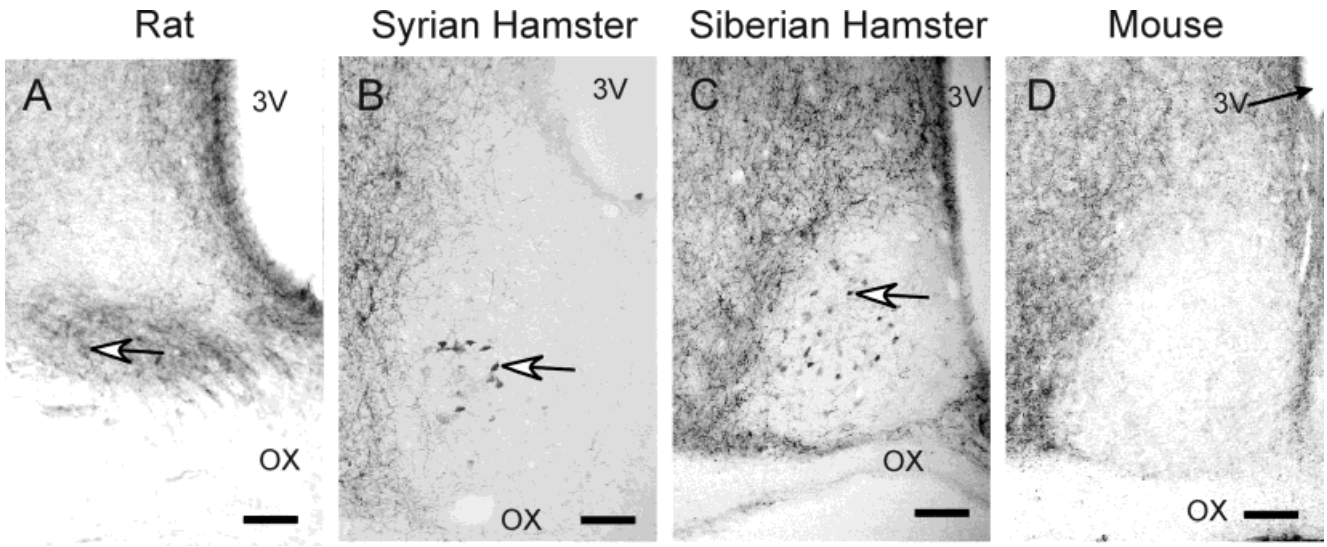

Fig. 2. High-power photomicrographs showing SP immunostaining of cells (white arrows) in the rodent SCN. Note faintly labelled cells in the rat (**A**), numerous darkly stained cells in the Syrian hamster (**B**) and Siberian hamster (**C**), and absence of immunostained cells in the mouse (**D**). Scale bars = 50 μm.

tricle also showed moderate SP-immunopositive terminal staining at all rostrocaudal levels of the SCN. Substance P-immunopositive fibres and terminals were sparse or absent from the SCN (Figs. 1E, 3C,G,K). Cells immunostained for SP were observed in the central region of the intermediate level of the SCN (Fig. 2C).

Moderate to intense NK-1-ir fibres and cells were seen in the AHA surrounding the SCN (Fig. 1F), but very few immunoreactive cells and fibres were observed in the SCN (Fig. 3C,G,K). Some immunopositive fibres from the AHA surrounding the dorsal SCN were found to extend into the SCN periphery. The NK-1-ir cells seen in the AHA were elliptical in shape and gave rise to one or two immunostained processes.

Mouse. Within the SCN, SP-ir terminals and fibres were sparse or absent at all rostrocaudal levels (Figs. 1G, 3D,H,L). Areas of intense terminal staining were seen throughout the rostrocaudal extent in the AHA dorsal and lateral to the SCN. Sparsely distributed SP-ir fibres were also seen in the AHA. Cells immunostained for SP were absent from the SCN (Fig. 2D) but were seen in the supraoptic nucleus and hypothalamic paraventricular nucleus (data not shown).

Deeply stained NK-1-ir fibres and cells were seen to surround the SCN in the AHA at all rostrocaudal extents, and some fibres extended into the periphery of the SCN from this region (Figs. 1H, 3D,H,L). The fibres looked irregular in appearance, with nodules along their lengths. Some NK-1-ir fibres and a small number of NK-1-ir cells were present in the dorsolateral SCN at intermediate rostrocaudal levels. The NK-1-ir cells observed in the AHA were mainly spherical in shape, with no obvious processes associated with them.

Intergeniculate leaflet

Rat. The lateral geniculate region exhibited moderately stained SP-ir terminals confined mostly to the IGL (Fig. 5A) throughout its rostrocaudal extent, with sparse immunolabelling in the lateral region of the dorsal lateral geniculate nucleus (dLGN). Sparse SP-ir fibre staining was also observed in the rostral and intermediate levels of the lateral region of the ventral lateral geniculate nucleus (vLGN), whereas sparse to moderate numbers of SP-ir fibres were found in the caudal aspects of the vLGN (Fig. 8A,E,I). Few varicosities were seen extending into the caudal levels of the medial vLGN. No SP-ir cell bodies were seen at any level of the lateral geniculate complex. At its most caudal level, SP-ir in the IGL became contiguous with SP-ir terminals and fibres in the zona incerta (ZI).

Fibres and soma darkly stained for NK-1 were observed throughout the rostrocaudal extent of the IGL. Sparse fibre staining was seen along the lateral border of the dLGN at intermediate to caudal levels. The fibres observed in the vLGN also contained varicosities. Fibre density increased rostrocaudally to cover the expanding IGL, until the IGL became contiguous with the ZI (Fig. 9A,E,I). Numerous NK-1-ir cell bodies were seen throughout the rostrocaudal extent of the IGL, with very few cells found in the vLGN. The NK-1-immunopositive cells were localized to the dorsolateral region of the IGL (Fig. 6A) and had one or two NK-1-ir processes associated with them. Double-labelling for SP and the NK-1 receptor at the level of the IGL revealed SP-ir terminals in close proximity to NK-1-ir perikarya and processes (Fig. 7A,B).

Syrian hamster. The visual thalamic region contained darkly stained SP-ir terminals, confined mainly to the IGL throughout the rostrocaudal extent. Substance P-immunopositive terminals were rare in the dLGN and were confined mainly to the lateral border of this structure, whereas little to no SP-ir was found in the vLGN. The density of terminals exhibiting immunopositive staining was moderate across the rostrocaudal extent of the IGL with some varicose SP-ir fibres seen in the caudal vLGN (Fig. 5B). No SP-ir cell bodies were seen at any level of the IGL, dLGN, or vLGN (Fig. 8B,F,J).

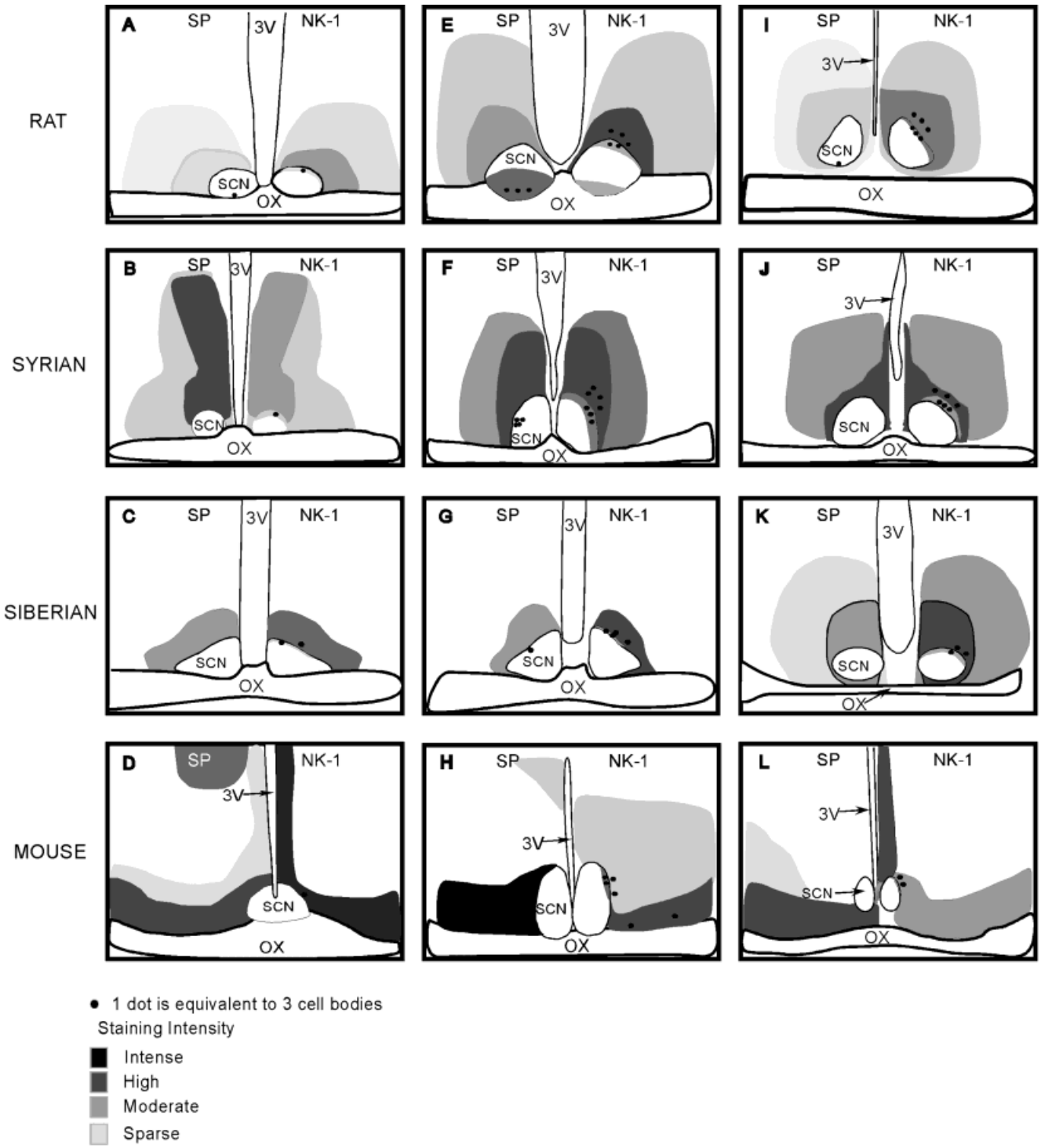

Fig. 3. Diagrammatic representations of the distribution and intensity of SP (left-hand side of each panel) or NK-1 (right-hand side of each panel) immunostaining at rostral (**A–D**), intermediate (**E–H**), and caudal (**I–L**) levels of the SCN in rat (A,E,I), Syrian hamster (B,F,J), Siberian hamster (C,G,K), and mouse (D,H,L).

Fibres immunostained for the NK-1 receptor were abundant throughout the rostrocaudal extent of the IGL and were present at the caudal aspect, as it becomes contiguous with the ZI. The density of NK-1-ir fibres was sparse in the vLGN and absent in the dLGN (Fig. 6B). The number of NK-1-ir neurones increased in a rostrocaudal

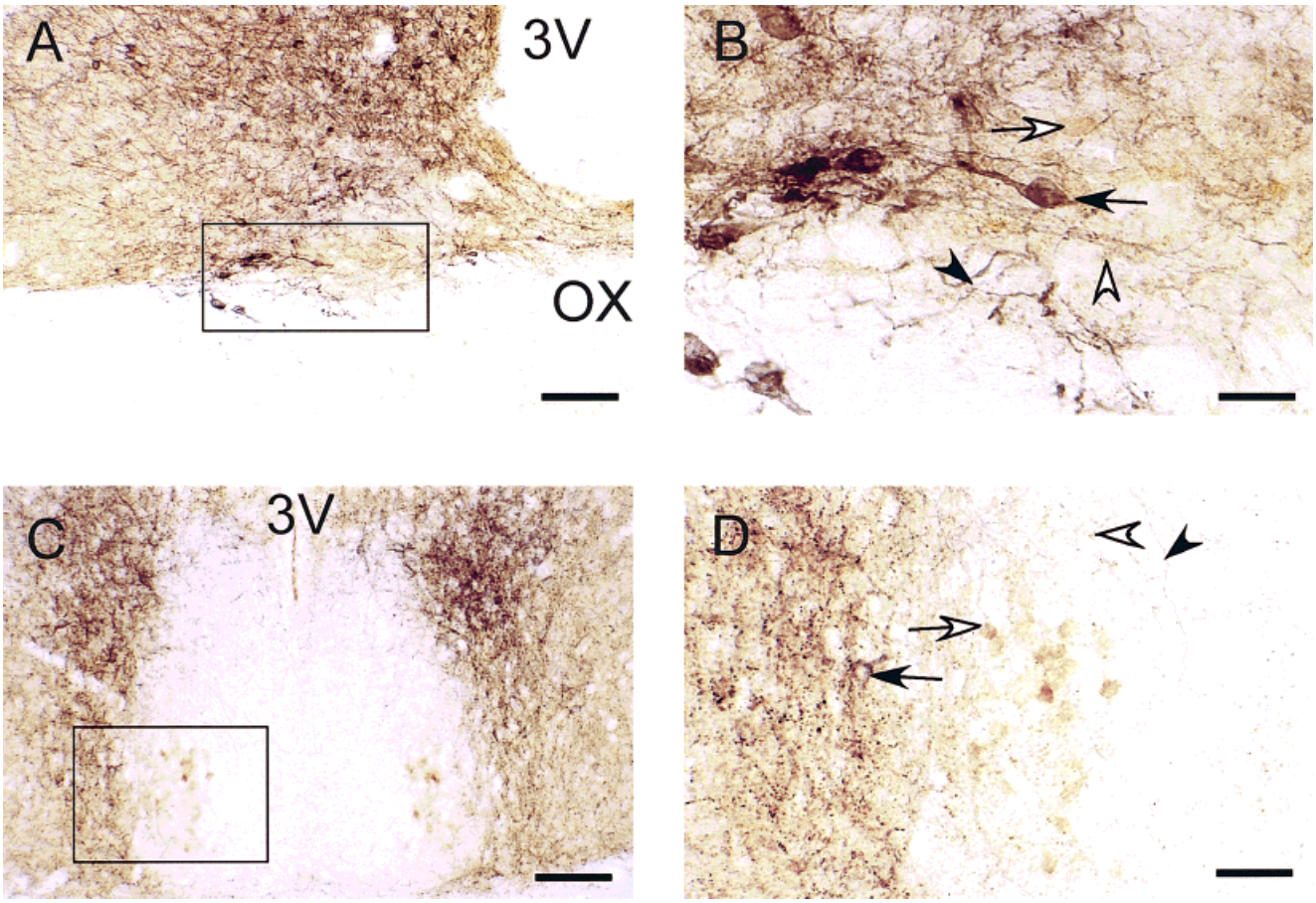

Fig. 4. Low- (**A**,**C**) and high-power (**B**,**D**) photomicrographs showing the SCN of rat (A,B) and Syrian hamster (C,D) double-immunostained for SP (brown reaction product) and NK-1 (purple reaction product). The regions delineated in A and C are shown at higher magnification in B and D, respectively. Note the presence of SP-ir terminals (white-filled arrowheads) in proximity to NK-1-ir cells (black-filled arrows) and processes (black-filled arrowheads) in both rat and Syrian hamster SCN. Note also the presence of SP-ir cell bodies (white-filled arrows) in the SCN region of both species. Scale bars = 100 μm in A,C, 25 μm in B, 40 μm in D.

direction, reflecting the changing shape of the IGL (Fig. 9B,F,J). In IGL sections double-labelled for SP and NK-1, SP-ir terminals could be observed overlapping NK-1-ir cells and dendrites (Fig. 7C,D), suggesting that locally released SP could act on these NK-1-immunopositive IGL cells.

Siberian hamster. In the visual thalamus, a moderate to high density of SP-ir terminal staining was observed throughout the rostrocaudal extent of the IGL (e.g., intermediate IGL; Fig. 5C). A few fibres were found in the IGL, but a larger number were located at caudal aspects of the vLGN region. These fibres had a fine appearance with larger swellings along their lengths (Fig. 5E). SP-ir was absent from the dLGN. No SP-ir cells were seen throughout the rostrocaudal extent of the IGL, vLGN, or dLGN (Fig. 8C,G,K).

The intensity of NK-1-ir staining varied throughout the rostrocaudal extent of the IGL. Sparse numbers of fibres and cells were observed rostrally, but numbers of both increased in the intermediate (Fig. 6C,E) and caudal levels of the IGL to cover the expanding shape of the IGL. Cells expressing NK-1-ir were mainly spherical in appearance and concentrated in the lateral portion of the IGL. Prominent NK-1-ir fibre staining was seen in the ZI as the intensely stained caudal IGL becomes contiguous with this structure (data not shown). Immunopositive NK-1 staining was absent from the dLGN, whereas some NK-1-ir staining, mostly on fibres, was found in the lateral vLGN (Fig. 9C,G,K).

Mouse. Within the visual thalamus, darkly stained SP-immunopositive terminals of moderate density were observed throughout the rostrocaudal extent of the IGL. Some SP-ir fibres were seen in the vLGN (Fig. 5D). Substance P-ir was absent from all levels of the dLGN. No SP-immunostained cells were observed in any aspects of the dLGN, IGL, or vLGN (Figs. 5F, 8D,H,L).

Neurokinin-1-immunopositive staining in the IGL was found to be predominantly fibrous. The fibres were deeply stained and uneven in appearance with nodules along their length. Neurokinin-1-ir cell bodies were sparse and only detected at intermediate levels of the IGL amongst very dense NK-1-ir fibres (Fig. 6F). Fibrous staining was high throughout the rostrocaudal extent of the IGL until this structure became contiguous

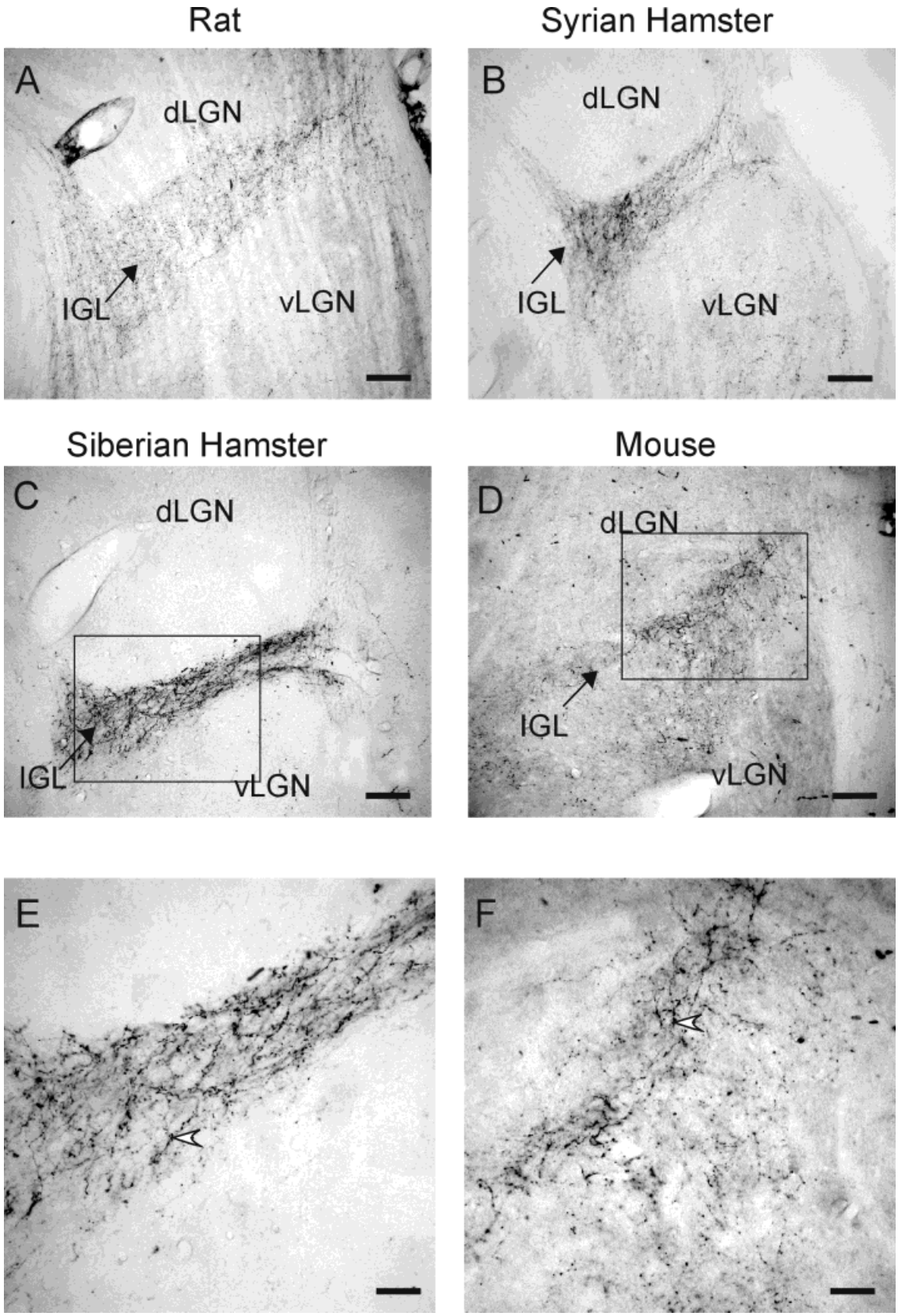

Fig. 5. Low- and high-power photomicrographs showing the pattern of SP immunostaining at the intermediate level of the intergeniculate leaflet (IGL) of the rat (**A**), Syrian hamster (**B**), Siberian hamster (**C**,**E**), and mouse (**D**,**F**). SP-ir terminals are indicated by white-filled arrowheads. Scale bars = 70 μm in A, 100 μm in B, 60 μm in C, 50 μm in D, 35 μm in E, 30 μm in F.

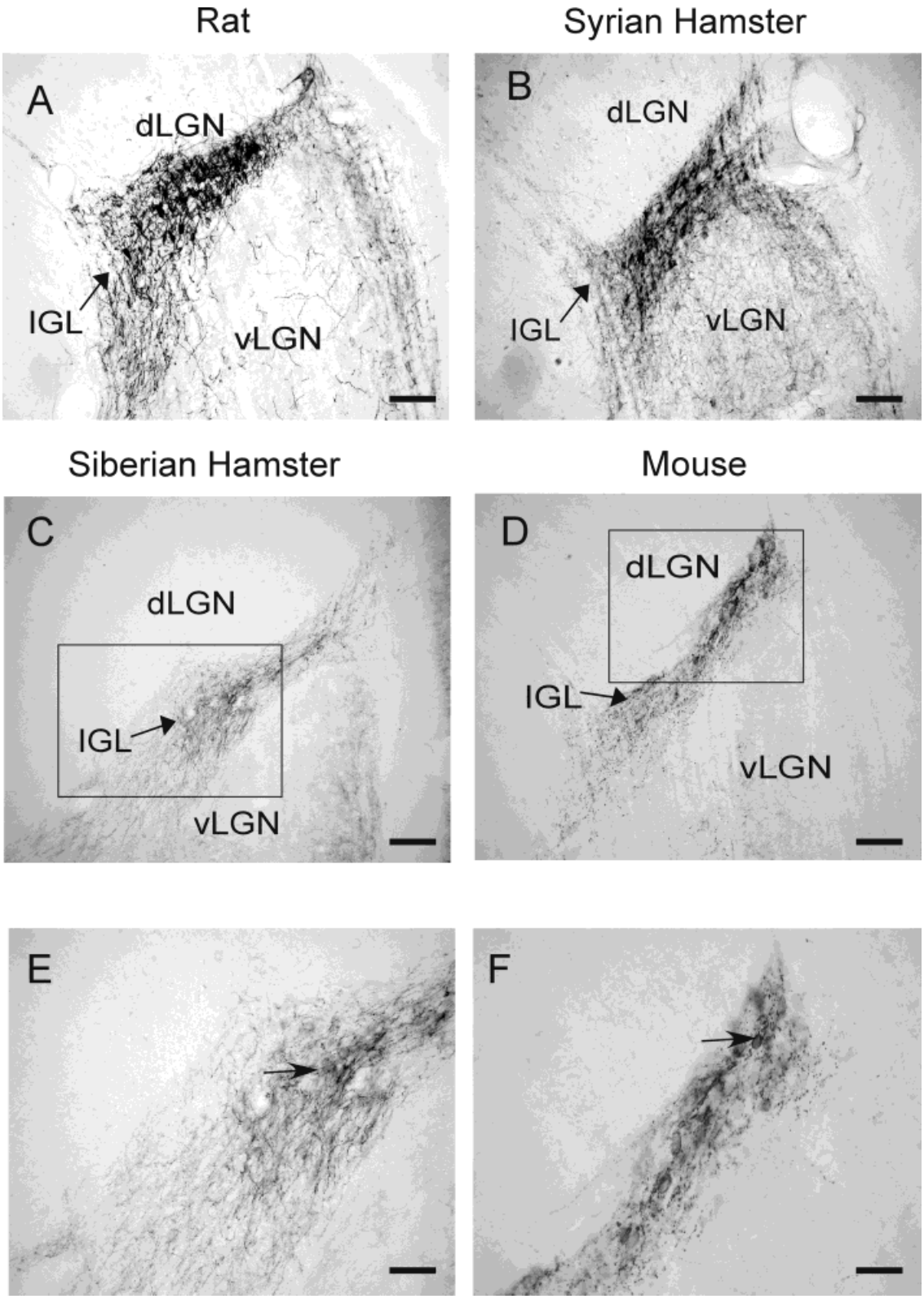

Fig. 6. Low- and high-power photomicrographs showing the pattern of NK-1 immunostaining at the intermediate level of the IGL of the rat (**A**), Syrian hamster (**B**), Siberian hamster (**C**,**E**), and mouse (**D**,**F**). NK-1-ir cell bodies are indicated by dark-filled arrows in E and F. Scale bars = 65 μm in A,B, 50 μm in C, 55 μm in D, 25 μm in E,F.

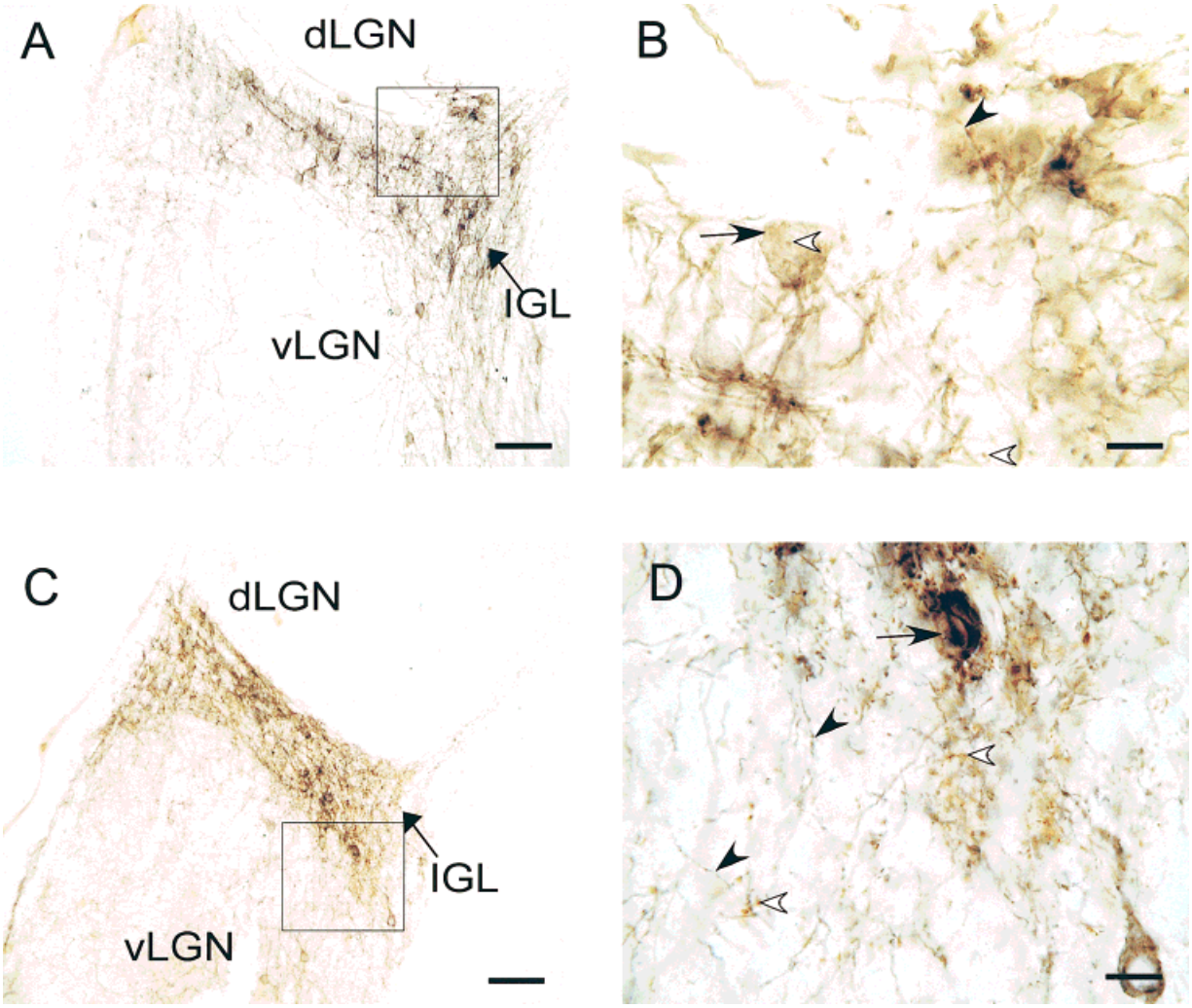

Fig. 7. Low- (A,C) and high-power (B,D) photomicrographs showing the rat (**A**,**B**) and Syrian hamster IGL (**C**,**D**) double-immunostained for SP (brown reaction product) and NK-1 (purple reaction product). The areas delineated in A and C are shown at higher magnification in B and D, respectively. In these panels, note the presence of SP-ir terminals (white-filled arrowheads) in close proximity to NK-1-ir cells (black-filled arrows) and processes (black-filled arrowheads) in both rat and Syrian hamster IGL. Scale bars = 75 μm in A,C, 15 μm in B,D.

with the ZI (data not shown). No NK-1-ir staining was found in the dLGN, but a few darkly stained varicosities were distributed in the dorsal region of the vLGN (Figs. 6D, 9D,H,L).

Controls

Preadsorption of either the SP monoclonal antibody or the SP polyclonal antiserum with SP abolished immunostaining in the SCN and IGL regions of all species. Similarly, preadsorption of the NK-1 antisera with the peptide sequence KTMTESSSFYSNMLA, corresponding to the 393–407 amino acids of the receptor C-terminus, completely blocked immunostaining to this antiserum in the SCN and IGL of all species. Omission of the primary antisera or secondary antibody also abolished immunostaining to these antigens.

DISCUSSION

Immunoreactivity for SP and NK-1 was found in the SCN and IGL regions of all four species investigated, although interspecies differences in the pattern and intensities of immunostaining were found (see below). The patterns of immunostaining for NK-1 in the IGL and SCN of the rat and Syrian hamster found in this study are consistent with those observed earlier by Nakaya et al. (1994) and Mick et al. (1995). They reported the presence of NK-1-immunopositive cells and fibres in the IGL of both species. They also found that NK-1-ir was more intense along the dorsal and lateral borders of the SCN of both species, rather than within the SCN. Our findings extend the knowledge of the distribution of SP, and in particular the NK-1 receptor, in some key structures of the rodent circadian system. Specifically, these results show that NK-1-ir is readily detectable in the hypo-

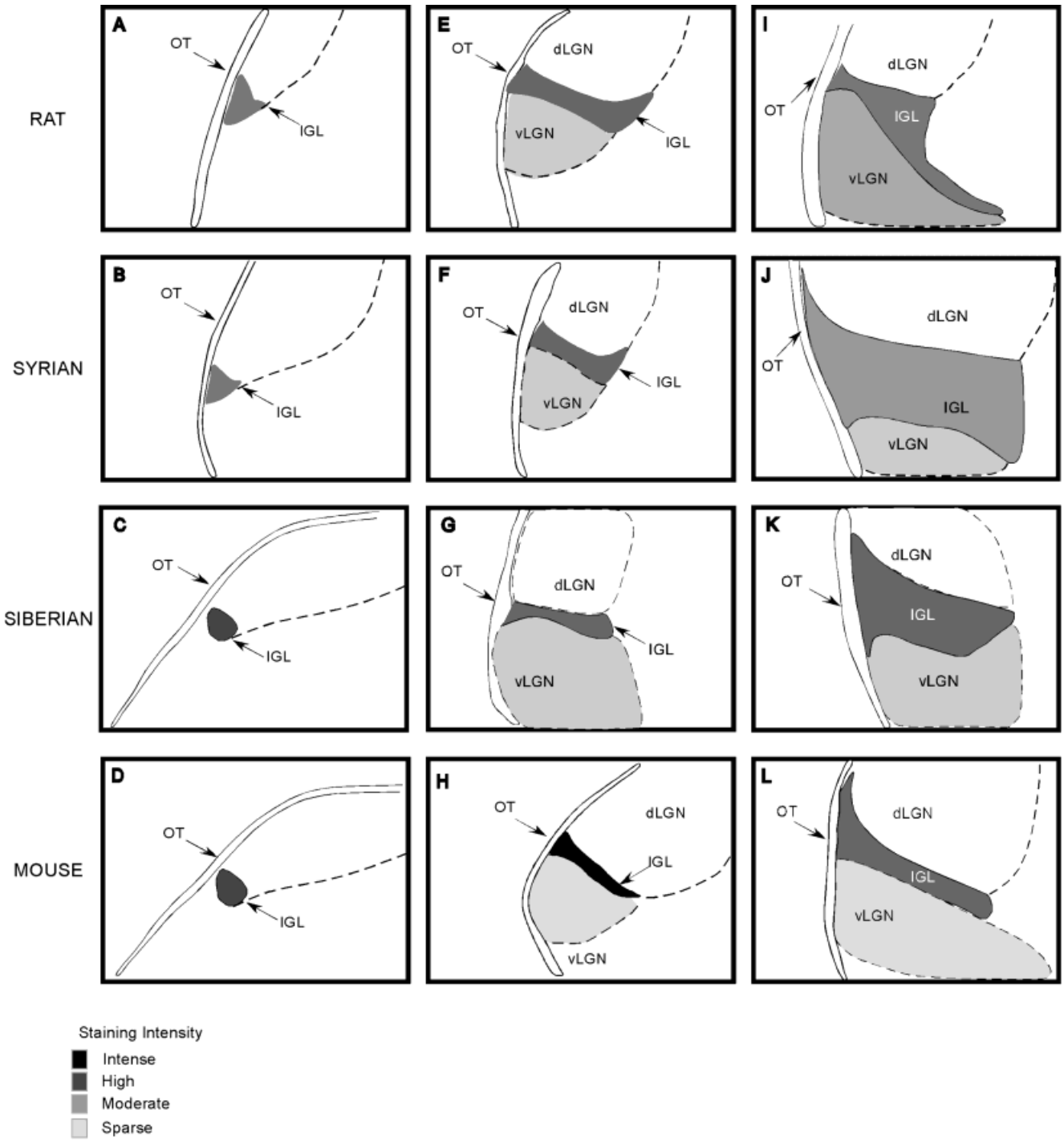

Fig. 8. Diagrammatic representation of the distribution and intensity of SP immunostaining at the rostral (**A–D**), intermediate (**E–H**), and caudal (**I–L**) levels of the IGL in rat (A,E,I), Syrian hamster (B,F,J), Siberian hamster (C,G,K), and mouse (D,H,L).

thalamus and thalamus of the Siberian hamster and mouse, and they indicate a remarkable conservation in the patterns of immunostaining for SP and NK-1 in the SCN and IGL of three of the four species. The intensity and robustness of the NK-1 immunostaining in the rodent IGL suggests that this is a very useful neurochemical marker for this specialized structure of the visual thalamus. The absence of SP-ir terminals in the ventral retinally innervated portion of the SCN in three of the four species indicates that the role of SP in regulating the SCN circadian clock probably differs in rat compared with Syrian and Siberian hamster and mouse (see below).

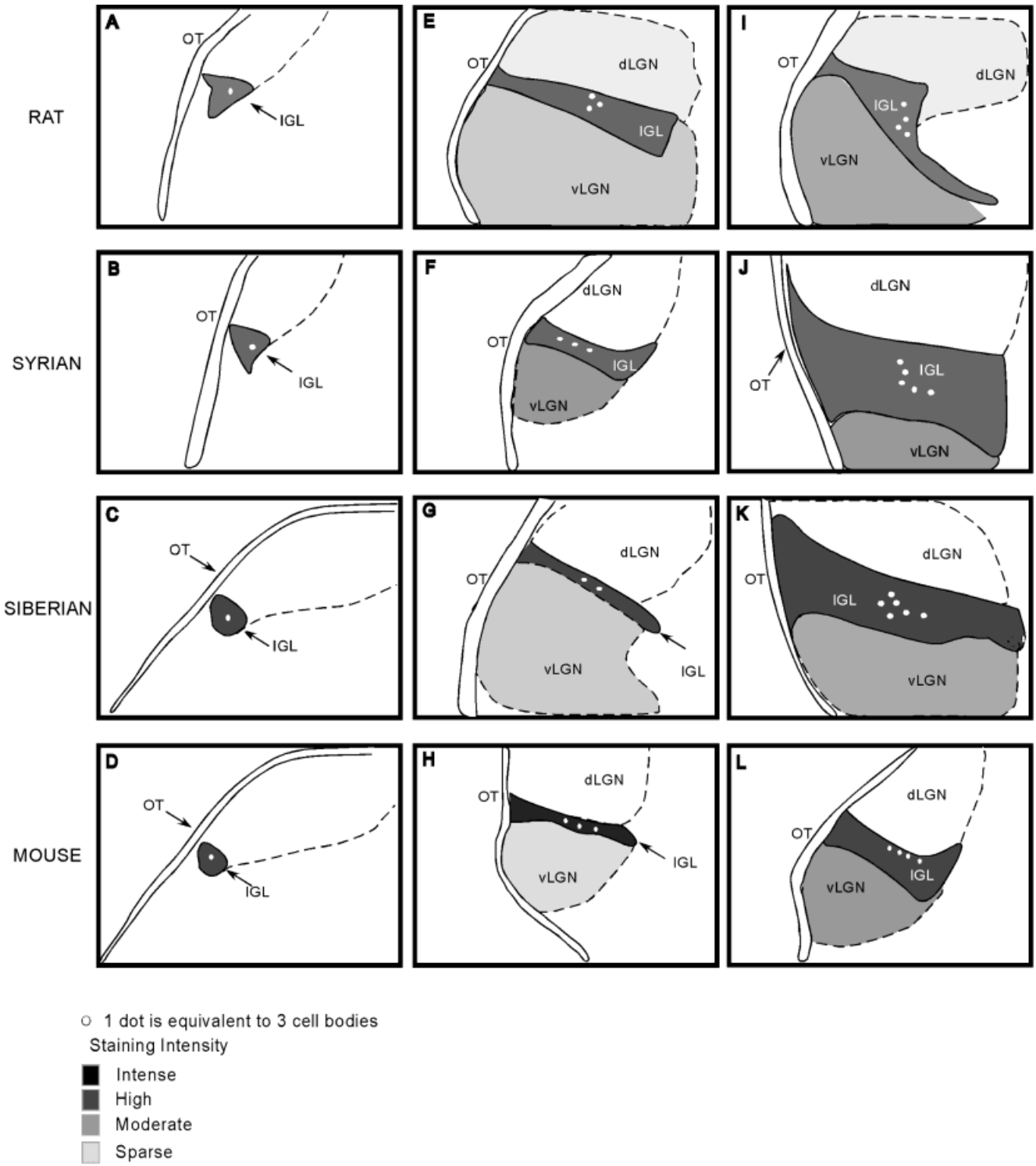

Fig. 9. Diagrammatic representation of the distribution and intensity of NK-1 immunostaining at the rostral (**A–D**), intermediate (**E–H**), and caudal (**I–L**) levels of the IGL in rat (A,E,I), Syrian hamster (B,F,J), Siberian hamster (C,G,K), and mouse (D,H,L).

Suprachiasmatic nuclei

In all species, both SP-ir and NK-1-ir was intense in the hypothalamic regions adjacent to the SCN. However, at the level of the SCN, the pattern of immunostaining varied considerably between rat and the other three species. In rat, SP-ir fibres and terminals were present in the

ventral SCN, whereas SP-ir terminals only sparsely innervated the dorsal SCN. Cell bodies immunopositive for SP were seen scattered throughout both the dorsal and ventral divisions of the rat SCN. This pattern of SP-ir in the rat SCN is in general agreement with that reported previously (Cuello and Kanazawa, 1978; Ljungdahl et al., 1978; Watts and Swanson, 1987; Larsen, 1992; Hartwich et al., 1994). Immunostaining for NK-1 was confined mainly to a small but intensely stained plexus of fibres within the ventrolateral division of the rat SCN, whereas the dorsal SCN contained sparse NK-1-ir fibre labelling. Double-labelling of the rat SCN with SP and NK-1 revealed numerous SP-ir terminals in close proximity to the intensely labelled NK-1 fibres and cell bodies in the ventrolateral SCN, implying that NK-1-ir elements are innervated by SP-containing terminals. Takatsuji and colleagues (1995) determined that RHT terminals synapsed on NK-1-ir elements in the rat SCN, and further electron microscopy studies are required to determine whether SP is contained in these RHT terminals contacting NK-1-ir cellular processes in the rat ventrolateral SCN.

In contrast to these findings in rat, SP-ir fibre staining was largely sparse or absent from the SCN of Syrian and Siberian hamsters and the mouse, in accordance with previous reports on these species (Stoeckel et al., 1982; Morin et al., 1992; Reuss and Bürger, 1994; Silver et al., 1999). The paucity of SP-ir fibres/terminals in the retinally innervated region of the SCN of hamsters and mouse argues against the possibility that SP is a key RHT neurotransmitter conveying photic information in these species. Consistent with this interpretation, NK-1-ir cells and dendrites were mostly absent from the ventral SCN of all three species. As with SP-ir, NK-1 receptor immunostaining was much greater along the dorsolateral borders of the SCN and in adjacent hypothalamic regions. In all of these species, NK-1-ir cells were found in the transition zone between the SCN and AHA, whereas some NK-1-ir dendrites were present in the core of the SCN. These findings suggest that the likely neuroanatomical site of action of SP within the SCN region of mouse and hamsters is on these dendritic processes that arise from NK-1-ir cells along the dorsolateral border of the SCN. Examination of Syrian hamster hypothalamic sections that were double-labelled for SP and the NK-1 receptor supports this interpretation, because SP-ir terminals appeared in close proximity with NK-1-ir cell bodies and processes in the dorsolateral borders of the SCN. Electron microscopy studies are required to determine whether SP is contained in synaptic terminals in apposition to these NK-1-ir cells and cellular processes.

Functional studies of the role of SP in the SCN circadian clock in hamsters have been inconclusive. Abe and colleagues (1996) found that infusions of spantide, a broad-spectrum SP receptor antagonist, into the lateral ventricles blocked light-evoked increases in the expression of the immediate early gene protein product Fos in the hamster SCN. The site of action of spantide in this study remains unclear because the known pharmacology of spantide indicates that this compound can act on a number of receptor types. This raises the possibility that the actions of spantide on the photic regulation of gene expression in the hamster SCN could be upstream of the SCN and via as yet uncharacterized receptors. However, Piggins and Rusak (1997) found that microinjection of SP directly into the SCN region of hamsters free-running in constant conditions did not significantly alter the phase of this wheel-running rhythm. This suggests that SP does not play a key role in resetting the Syrian hamster SCN circadian clock. Furthermore, the absence of significant immunostaining for SP or NK-1 in the SCN of mouse and Siberian hamster indicates that SP is unlikely to be a major neurotransmitter of the RHT in these species.

In the rat, results from in vitro studies support the contention that SP functions as an important neurochemical of the RHT. Extracellular recordings from spontaneously discharging rat SCN neurones maintained in a brain slice in vitro have shown that SP predominantly activates rat SCN neurones (Shibata et al., 1992; Shirakawa and Moore, 1994) and that these effects are blocked by spantide. Furthermore, SP has been shown to phase-reset the electrical and metabolic rhythms of rat SCN neurones in vitro in a manner resembling the phase-shifting actions of light pulses on rodent behavioural rhythms (Shibata et al., 1992). These phase-resetting effects were also blocked by spantide. A limitation of these experiments is that spantide, as mentioned above, is not selective for tachykinin receptors and has neurotoxic properties that confound interpretation of these results. However, a recent in vitro electrophysiological investigation using the selective NK-1 receptor antagonist L-703,606 found that this compound attenuated the excitatory effects of optic nerve stimulation on a population of (presumptive) retinorecipient rat SCN cells (Kim et al., 1999), suggesting that activation of the optic nerve releases SP from rat RHT terminals. Furthermore, it has been found that SP-induced phase shifts in the electrical firing rate rhythm of rat SCN neurones in vitro are attenuated by an ionotropic glutamate receptor antagonist (Hamada et al., 1999), indicating that SP requires functional ionotropic glutamate receptors in order to elicit maximal phase shifts. A possible explanation of these findings is that SP and glutamate are co-released from RHT terminals to modulate each other's actions on retinorecipient SCN cells. The results of our study showing SP-ir terminals in the rat ventral SCN, together with intensely stained NK-1-ir cell bodies and fibres in the retinally innervated ventrolateral division of the SCN, support the assertion that SP functions as an RHT neurotransmitter conveying photic information to the SCN in this species.

Despite these strong functional data that favour the proposition that SP is contained in the rat RHT, supporting neuroanatomical evidence is contentious. An early study combining tract-tracing and SP immunohistochemistry, indicated that SP-ir was present in the axons of retinal ganglion cells that projected to the rat SCN (Takatsuji et al., 1991). This group also found that bilateral optic enucleation significantly attenuated SP-ir fibre labelling in the rat SCN, an observation confirmed by Mikkelsen and Larsen (1993). However, two independent studies (Otori et al., 1993; Hartwich et al., 1994) could not detect differences in the patterns of SP-ir immunostaining in the rat SCN between blinded and sham operated controls. The disparities in the results of these studies may be attributable to differences in the length of time following blinding that SP-ir was investigated, immunohistochemical procedures, or the SP antisera employed. Because we found similar patterns of SP-ir staining in the rat SCN with both a monoclonal antibody to SP and a commercially available polyclonal antiserum to SP, differences in immunostaining observed in the above studies are most likely due to

differences in the duration of the postenucleation recovery phase. Further studies from other laboratories are necessary to determine the precise source of SP-ir innervation of the rat SCN.

In hamsters and rat, cells immunopositive for SP were found within the SCN. This indicates that colchicine treatment is not necessary to detect SP-containing cells in the SCN of these species. In Siberian and Syrian hamsters, the SP cells were darkly labelled, whereas in the rat, cell bodies were lightly stained. Previous researchers have noted that colchicine treatment does not increase the number of SP-ir cells in the Syrian hamster SCN, although the intensity of staining does increase (Morin et al., 1992). In the rat, two groups (Ljungdahl et al., 1978; Larsen, 1992) detected SP-ir cells in the SCN in colchicine-treated rats, but not in untreated animals. Because we found lightly stained neurones in the SCN of untreated rats, it is likely that differences in immunohistochemical and fixation procedures account for the apparent discrepancies between our results and those of other researchers. We could not find SP-ir cells in the SCN of the mouse. It is unknown whether colchicine pretreatment would have enabled detection of SP-immunopositive cells in the C57BL/6xSV129 mouse SCN, but SP-ir soma were not seen in the SCN with colchicine pretreatment in a different strain of mouse (Stoeckel et al., 1982).

In both Siberian and Syrian hamsters, SP-ir soma were limited to the central region of the intermediate level of the SCN, a pattern consistent with that reported in previous studies (Morin et al., 1992; Hartwich et al., 1994; Reuss and Bürger, 1994). Because some of these SP-ir perikarya lie within the retinally innervated region of the hamster SCN, it is likely that RHT terminals (Reuss et al., 1994) contact them. In the rat, we also detected faintly labelled SP-ir cells scattered throughout the SCN. As with the hamster SCN, some of these SP-immunopositive cells lay in the retinally innervated portion of the SCN, suggesting that they may be retinorecipient cells. Further studies are required to verify that retinal afferents directly contact SP-containing cells in the SCN of these species.

Substance P-immunostaining within the SCN also varies across other mammalian species. For example, in the human, a plexus of SP-ir fibres has been found in the retinally innervated portion of the SCN, suggesting that SP is contained in the RHT of this species (Mai et al., 1991; Moore and Speh, 1994). In the non-human primate *Macaca fascicularis*, SP-ir neurones and fibres are found in the dorsal SCN, whereas the ventral division is largely devoid of SP immunostaining (Mick et al., 1992). In some rodents such as *Octodon degus*, *Arvicanthis niloticus*, and *Spermophilus lateralis*, SP-ir fibres are sparse or absent within the retinally innervated areas of the SCN but instead are found in high intensities in the anterior hypothalamic area adjacent to the SCN (Smale et al., 1991; Goel et al., 1999; Smale and Boverhof, 1999). Substance P-immunopositive cells were either very few in number or not detected in the SCN in *Arvicanthis niloticus* and *Spermophilus lateralis*, even following colchicine pretreatment. From these immunohistochemical studies, it would appear that SP is not synthesized by SCN cells in *Arvicanthis niloticus* or *Spermophilus lateralis* and that SP is unlikely to be an RHT transmitter in these species. The pattern of NK-1-ir in the SCN of these species has not been reported, but preliminary evidence from our laboratory indicates that NK-1-ir soma and dendrites are found along the dorsal and lateral borders of the degu SCN (Piggins and Samuels, unpublished observations), suggesting that the distribution of NK-1-ir at the level of the SCN is similar in many rodent species.

Intergeniculate leaflet

The pattern of immunostaining for both SP and NK-1 was similar in the IGL of the rat, mouse, and Siberian and Syrian hamster. Immunoreactive SP fibres and terminals were present throughout the rostrocaudal extent of the IGL of all species. In contrast, SP-ir fibres were sparse or absent in the dLGN and sparse in the vLGN. These results are in broad agreement with studies of the distribution of SP in the mammalian visual thalamus in which SP-ir terminals were found in the IGL of cat, rabbit, Syrian hamster, and rat (Brecha et al., 1987; Battaglia et al., 1992; Morin et al., 1992; Kalsbeek et al., 1993; Moore and Card, 1994).

In the IGL of the rat, mouse, and Siberian and Syrian hamster, NK-1-ir was present throughout the rostrocaudal extent. The finding that NK-1-ir is intense in the rat IGL is consistent with previous studies on this species localizing the NK-1 receptor by immunohistochemistry (Mick et al., 1995) and in situ hybridization techniques (Maeno et al., 1993; Mick et al., 1994) to the IGL. Furthermore, a receptor autoradiography study using [^{3}H]SP has described moderate binding in the rat IGL (Mantyh et al., 1984). Collectively, these studies show that cells in the rat IGL express the NK-1 receptor. Although information on NK-1 distribution is limited in hamster and mouse, Mick and colleagues (1995) showed intense NK-1-ir in the IGL of the Syrian hamster.

In all species examined in this study, NK-1 receptor immunostaining was largely limited to the IGL, with very few varicotic fibres seen in the dLGN area immediately dorsal to the IGL, and a low to moderate density of NK-1-ir in the lateral and medial divisions of the vLGN. (In all species examined, immunostaining for NK-1 was more prevalent in the caudal vLGN than in rostral or intermediate sections.) The intensity of NK-1 immunostaining showed interspecies variation, with the most intense immunolabelling seen in the rat and mouse. Less intense NK-1-ir was observed in the IGL of the Siberian and Syrian hamsters. In rostral IGL sections from all species, NK-1-ir staining appeared to be confined to a network of fibres. However, in intermediate and caudal levels, intensely stained cell bodies were observed in the IGL and occasionally, in the vLGN. These soma were more readily observed in the rat and mouse IGL, although lightly stained NK-1-immunopositive cell bodies were found in the IGL of the Syrian and Siberian hamsters. In the rat and hamster IGL, these immunopositive cells gave rise to one or two immunolabelled fibre processes that appeared to be confined to the boundaries of the NK-1-ir within the IGL. However, in some instances, these fibres coursed dorsally into the dLGN. This pattern of NK-1-ir suggests that much of this immunostaining in the lateral geniculate complex arose from neurones within the IGL.

The reasons for the interspecies variation in the intensity of NK-1-ir in the IGL are unclear. It is possible that there are small differences in the amino acid sequence of the NK-1 receptor between the species, particularly in the Siberian hamster, and that these subtle differences alter the antigenicity of the receptor. This is necessarily spec-

ulative as the NK-1 receptor has not been cloned and sequenced in Siberian and Syrian hamsters. Previous investigations have revealed that at least two isoforms of the NK-1 receptor are present in mammals (Fong et al., 1992). Furthermore, a recent radioligand study has demonstrated two subtypes of NK-1 receptor binding sites in the rat central nervous system (Beaujouan et al., 2000). It is possible that different isoforms of NK-1 receptor may be expressed differentially in the IGL of the species examined. It is unknown whether the antiserum to the NK-1 receptor used in this study recognizes the epitopes of some or all of these NK-1 isoforms. Our observation that preincubation with the 393–407 amino acid sequence from the C-terminus of the NK-1 receptor abolished all immunostaining in the CNS of all the species examined suggests that this sequence is conserved in the isoforms of the NK-1 receptor that may be found in these species. Further studies using antisera raised to specific NK-1 receptor isoforms are required to test for this possibility.

The double-labelled sections from rat and Syrian hamster IGL showing SP-ir terminals in close proximity to NK-1-labelled cells and dendrites suggest that SP released from these terminals could act to alter the activity of IGL neurones. The source(s) of this SP innervation are unknown, but likely candidates include the dorsal raphe and subcortical visual structures, because these sites are known to innervate the rodent IGL (Meyer-Bernstein and Morin, 1996; Morin and Blanchard, 1998; Marchant and Morin, 1999). It is unlikely that SP-ir fibres and terminals in the rodent IGL originate in the retina, as Miguel-Hidalgo and colleagues (1991) previously showed that bilateral optic enucleation does not reduce SP-ir in this region of the rat visual system. Tract-tracing studies combined with SP immunohistochemistry are required to determine the precise origins of the SP innervation of the rodent IGL.

Although a previous study reported the presence of SP-ir cells in the IGL of colchicine-treated rats (Takatsuji and Tohyama, 1989), no SP-ir cells were found in the IGL of any species studied in the present investigation. Because other researchers have also failed to detect SP-ir cells in the IGL of colchicine-treated rats (Ljungdahl et al., 1978; Mantyh and Kemp, 1983; Moore and Card, 1994), this suggests that either SP is not found in rat IGL cells or that the detection of SP-ir in these neurones is contingent on immunohistochemical procedures. In other rodents such as the Syrian hamster (Morin et al., 1992; Hartwich et al., 1994) or *Spermophilus lateralis* (Smale et al., 1991), SP-immunopositive cells were not found in the IGL of colchicine-treated animals. These data indicate that SP is unlikely to be synthesized by rodent IGL neurones.

The role of SP in the IGL is unknown. A previous study by Challet and colleagues (1998) showed that peripheral injection of the NK-1 receptor antagonist L760,735 phase-dependently phase-advanced Syrian hamster wheel-running rhythms in a manner resembling the actions of nonphotic stimuli. Furthermore, they found that these injections attenuated the phase-shifting effects of light on Syrian hamster behavioural rhythms. Previous studies have implicated the IGL in playing a pivotal role in relaying nonphotic information to the SCN (Mrosovsky, 1996; Harrington, 1997; Piggins and Rusak, 1999). Because NK-1-ir is largely absent from the Syrian hamster SCN, but is readily detectable in the IGL, it is possible that the NK-1 receptor antagonist acts via IGL neurones modulating the level of GHT activation, which in turn, regulates the phase of the SCN circadian clock. Alternatively, the antagonist may act on the NK-1-ir cells in the peri-SCN region that may project into the core of the SCN. Further functional experiments in vivo are required to elucidate the site(s) of action of NK-1 antagonists in the regulation of the behavioural rhythms of Syrian hamsters.

In summary, we found that the pattern of immunostaining for SP and the NK-1 receptor in the SCN was similar in the Syrian and Siberian hamsters and mouse but notably different in the rat. These neuroanatomical differences imply that SP has different roles in circadian clock function in the rat, compared with these other rodent species. In the IGL, both SP-ir and NK-1-ir was similar across all four species, suggesting that the actions of SP in this structure are well conserved across many rodent species.

ACKNOWLEDGMENTS

H.D.P. was the recipient of operating grants from the MRC (G962293N) and BBSRC (34/S12011). We thank Janet Small for her technical assistance.

LITERATURE CITED

Abe H, Rusak B. 1994. Physiological mechanisms regulating photic induction of Fos-like protein in hamster suprachiasmatic nucleus. Neurosci Biobehav Rev 18:531–536.

Abe H, Honma S, Shinohara K, Honma K-I. 1996. Substance P receptor regulates the photic induction of Fos-like protein in the suprachiasmatic nucleus of Syrian hamster. Brain Res 708:135–142.

Battaglia G, Spreafico R, Rustioni A. 1992. Substance P innervation of the rat and cat thalamus. I. Distribution and relation to ascending spinal pathways. J Comp Neurol 315:457–472.

Beaujouan J-C, Saffroy M, Torrens Y, Glowinski J. 2000. Different subtypes of tachykinin NK_1 receptor binding sites are present in the rat brain. J Neurochem 75:1015–1026.

Brecha N, Johnson D, Bolz J, Sharma S, Parnavelas JG, Lieberman AR. 1987. Substance P-immunoreactive retinal ganglion cells and their central axon terminals in the rabbit. Nature 327:155–158.

Castel M, Belenky M, Cohen S, Ottersen OP, Storm-Mathisen J. 1993. Glutamate-like immunoreactivity in retinal terminals of the mouse suprachiasmatic nucleus. Eur J Neurosci 5:368–381.

Challet E, Naylor E, Metzger JM, MacIntyre DE, Turek FW. 1998. An NK_1 receptor antagonist affects the circadian regulation of locomotor activity in golden hamsters. Brain Res 800:32–39.

Cuello AC, Kanazawa I. 1978. The distribution of substance P immunoreactive fibers in the rat nervous system. J Comp Neurol 178:129–156.

de Vries MJ, Nunes Cardozo B, van der Want J, de Wolf A, Meijer JH. 1993. Glutamate immunoreactivity in terminals of the retinohypothalamic tract of the brown Norwegian rat. Brain Res 612:231–237.

Ebling FJP. 1996. The role of glutamate in the photic regulation of the suprachiasmatic nucleus. Prog Neurobiol 50:109–132.

Fong TM, Anderson SA, Yu H, Huang RR, Strader CD. 1992. Differential activation of intracellular effector by two isoforms of human neurokinin-1 receptor. Mol Pharmacol 41:24–30.

Goel N, Lee TM, Smale L. 1999. Suprachiasmatic nucleus and intergeniculate leaflet in the diurnal rodent *Octodon degus*: retinal projections and immunocytochemical characterization. Neuroscience 92:1491–1509.

Hamada T, Yamanouchi S, Watanabe A, Shibata S, Watanabe S. 1999. Involvement of glutamate release in substance P-induced phase delays of suprachiasmatic neuron activity rhythm in vitro. Brain Res 836: 190–193.

Harrington ME. 1997. The ventral lateral geniculate nucleus and the intergeniculate leaflet: interrelated structures in the visual and circadian systems. Neurosci Biobehav Rev 21:705–727.

Hartwich M, Kalsbeek A, Pévet P, Nürnberger F. 1994. Effects of illumination and enucleation on substance-P-immunoreactive structures in subcortical visual centers of golden hamster and Wistar rat. Cell Tissue Res 277:351–361.

Hastings MH, Maywood ES. 2000. Circadian clocks in the mammalian brain. Bioessays 22:23–31.

Kalsbeek A, Teclemariam-Mesbah R, Pévet P. 1993. Efferent projections of the suprachiasmatic nucleus in the golden hamster (*Mesocricetus auratus*). J Comp Neurol 332:293–314.

Kim YI, Dudek FE. 1991. Intracellular electrophysiological study of suprachiasmatic nucleus neurons in rodents: excitatory synaptic mechanisms. J Physiol (Lond) 444:269–287.

Kim YI, Kim SH, Kim DY, Lee HW, Shin H-C, Chung J-M, Han HC, Na HS, Hong SK. 1999. Electrophysiological evidence for the role of substance P in retinohypothalamic transmission in the rat. Neurosci Lett 274:99–102.

Larsen PJ. 1992. Distribution of substance P-immunoreactive elements in the preoptic area and the hypothalamus of the rat. J Comp Neurol 316:287–313.

Ljungdahl Å, Hökfelt T, Nilsson G. 1978. Distribution of substance P-like immunoreactivity in the central nervous system of the rat - I. cell bodies and nerve terminals. Neuroscience 3:861–943.

Maeno H, Kiyama H, Tohyama M. 1993. Distribution of the substance P receptor (NK-1 receptor) in the central nervous system. Mol Brain Res 18:43–58.

Mai JK, Kedziora O, Teckhaus L, Sofroniew MV. 1991. Evidence for subdivisions in the human suprachiasmatic nucleus. J Comp Neurol 305: 508–525.

Mantyh P and Kemp JA. 1983. The distribution of putative neurotransmitters in the lateral geniculate nucleus of the rat. Brain Res 288:344–348.

Mantyh P, Hunt SP, Maggio JE. 1984. Substance P receptors: Localization by light microscopic autoradiography in rat brain using [^{3}H]SP as the radioligand. Brain Res 307:147–165.

Marchant EG, Morin LP. 1999. The hamster circadian rhythm system includes nuclei of the subcortical visual shell. J Neurosci 19:10482–10493.

Meyer-Bernstein EL, Morin LP. 1996. Differential serotonergic innervation of the suprachiasmatic nucleus and the intergeniculate leaflet and its role in circadian rhythm modulation. J Neurosci 16:2097–2111.

Mick G, Najimi M, Girard M, Chayvialle JA. 1992. Evidence for a substance P containing subpopulation in the primate suprachiasmatic nucleus. Brain Res 573:311–317.

Mick G, Maeno H, Kiyama H, Tohyama M. 1994. Marginal topography of neurons expressing the substance P receptor in the rat suprachiasmatic nucleus. Mol Brain Res 21:157–161.

Mick G, Shigemoto R, Kitahama K. 1995. Localization of substance P receptors in central neural structures controlling daily rhythms in nocturnal rodents. C R Acad Sci III 318:209–217.

Miguel-Hidalgo JJ, Senba E, Takatsuji K, Tohyama M. 1991. Effects of eye-enucleation of substance P-immunoreactive fibers of some retinorecipient nuclei of the rat in relation to their origin from the superior colliculus. Neuroscience 44:235–244.

Mikkelsen JD, Larsen PJ. 1993. Substance P in the suprachiasmatic nucleus of the rat: an immunohistochemical and in situ hybridization study. Histochemistry 100:3–16.

Moore RY, Card JP. 1994. Intergeniculate leaflet: an automatically and functionally distinct subdivision of the lateral geniculate complex. J Comp Neurol 344:403–430.

Moore RY, Speh JC. 1994. A putative retinohypothalamic projection containing substance P in the human. Brain Res 659:249–253.

Morin LP. 1994. The circadian visual system. Brain Res Rev 67:102–-127.

Morin LP, Blanchard JH. 1998. Interconnections among nuclei of the subcortical visual shell: the intergeniculate leaflet is a major constituent of the hamster subcortical visual system. J Comp Neurol 396:288–309.

Morin LP, Blanchard J, Moore RY. 1992. Intergeniculate leaflet and suprachiasmatic nucleus organization and connections in the golden hamster. Vis Neurosci 8:219–230.

Mrosovsky N. 1996. Locomotor activity and non-photic influences on circadian clocks. Biol Rev 71:343–372.

Nakaya Y, Kaneko T, Sigemoto R, Nakanishi S, Mizuno N. 1994. Immunohistochemical localization of substance P receptor in the central nervous system of the adult rat. J Comp Neurol 347:249–274.

Otori Y, Tominaga K, Fukuhara C, Yang J, Yamazaki S, Cagampang FRA, Okamura H, Inouye S-IT. 1993. Substance P-like immunoreactivity in the suprachiasmatic nucleus of the rat. Brain Res 619:271–277.

Paxinos G, Watson C. 1998. The rat brain in stereotaxic coordinates. San Diego: Academic Press.

Piggins HD, Rusak B. 1997. Effects of microinjections of substance P into the suprachiasmatic nucleus region on hamster wheel-running rhythms. Brain Res Bull 42:451–455.

Piggins HD, Rusak B. 1999. Intercellular interactions and the physiology of circadian rhythms in mammals. In: Lydic R, Baghdoyan HA, editors. Handbook of behavioural state control: cellular and molecular mechanisms. Boca Raton: CRC Press. p 31–44.

Piggins HD, Cutler DJ, Rusak B. 1995. Ionophoretically applied substance P activates hamster suprachiasmatic nucleus neurons. Brain Res Bull 37:475–479.

Ralph MR, Foster RG, Davis FC, Menaker M. 1990. Transplanted suprachiasmatic nucleus determines circadian period. Science 247:975–978.

Rea MA, Buckley B, Lutton LM. 1993. Local administration of EAA antagonists blocks light-induced phase shifts and c-fos expression in hamster SCN. Am J Physiol 265:R1191–1198.

Reuss S. 1996. Components and connections of the circadian system in mammals. Cell Tissue Res 285:353–378.

Reuss S, Bürger K. 1994. Substance P-like immunoreactivity in the hypothalamic suprachiasmatic nucleus of *Phodopus sungorus*—relation to daytime, photoperiod, sex and age. Brain Res 638:189–195.

Reuss S, Decker K, Hödl P, Sraka S. 1994. Anterograde neuronal tracing of retinohypothalamic projections in the hamster—possible innervation of substance P-containing neurons in the suprachiasmatic nucleus. Neurosci Lett 174:51–54.

Shibata S, Tsuneyoshi A, Hamada T, Tominaga K, Watanabe S. 1992. Effect of substance P on circadian rhythms of firing activity and the 2-deoxyglucose uptake in the rat suprachiasmatic nucleus in vitro. Brain Res 597:257–263.

Shirakawa T, Moore RY. 1994. Responses of rat suprachiasmatic nucleus neurons to substance P and glutamate in vitro. Brain Res 642:213–220.

Silver RL, LeSauter J, Tresco PA, Lehman MN. 1996. A diffusible coupling signal from the transplanted suprachiasmatic nucleus controlling circadian locomotor rhythms. Nature 382:810–813.

Silver RL, Sookhoo AI, LeSauter J, Stevens P, Jansen HT, Lehman MN. 1999. Multiple regulatory elements result in regional specificity in circadian rhythms of neuropeptide expression in mouse SCN. Neuroreport 10:3165–3174.

Smale L, Boverhof J. 1999. The suprachiasmatic nucleus and intergeniculate leaflet of *Arvicanthis niloticus*, a diurnal murid rodent from East Africa. J Comp Neurol 403:190–208.

Smale L, Blanchard J, Moore RY, Morin LP. 1991. Immunocytochemical characterization of the suprachiasmatic nucleus and intergeniculate leaflet in the diurnal ground squirrel, *Spermophilus lateralis*. Brain Res 563:77–86.

Stamp JA, Piggins HD, Rusak B, Semba K. 1997. Distribution of ionotropic glutamate receptor subunit immunoreactivity in the suprachiasmatic nucleus and intergeniculate leaflet of the hamster. Brain Res 756:215–224.

Stoeckel ME, Porte A, Klein MJ, Cuello AC. 1982. Immunocytochemical localization of substance P in the neurohypophysis and hypothalamus of the mouse compared with the distribution of other neuropeptides. Cell Tissue Res 223:533–544.

Takatsuji K, Senba E, Mantyh PW, Tohyama M. 1995. A relationship between substance P receptor and retinal fibers in the rat suprachiasmatic nucleus. Brain Res 698:53–61.

Takatsuji K, Tohyama M. 1989. The organization of the rat lateral geniculate body by immunohistochemical analysis of neuroactive substances. Brain Res 480:198–209.

Takatsuji K, Miguel-Hidalgo J-J, Tohyama M. 1991. Substance P-immunoreactive innervation from the retina to the suprachiasmatic nucleus in the rat. Brain Res 568:223–229.

van Esseveldt KE, Lehman MN, Boer GJ. 2000. The suprachiasmatic nucleus and the circadian time keeping system revisited. Brain Res Rev 33:34–77.

Watts AG, Swanson LW. 1987. Efferent projections of the suprachiasmatic nucleus: II. Studies using retrograde transport of fluorescent dyes and simultaneous peptide immunohistochemistry in the rat. J Comp Neurol 258:230–252.